Viscoelastic Properties of Human Bladder Tumours

S.C. Barnes, B.M. Lawless, D.E.T. Shepherd, D.M. Espino, G.R. Bicknell, R.T. Bryan

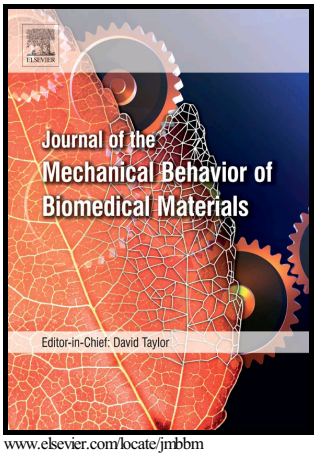

www.elsevier.com/locate/jmbbm

PII: S1751-6161(16)30032-7
DOI: http://dx.doi.org/10.1016/j.jmbbm.2016.03.012
Reference: JMBBM1845

To appear in: *Journal of the Mechanical Behavior of Biomedical Materials*

Received date: 26 January 2016
Revised date: 10 March 2016
Accepted date: 16 March 2016

Cite this article as: S.C. Barnes, B.M. Lawless, D.E.T. Shepherd, D.M. Espino G.R. Bicknell and R.T. Bryan, Viscoelastic Properties of Human Bladde Tumours, *Journal of the Mechanical Behavior of Biomedical Materials* http://dx.doi.org/10.1016/j.jmbbm.2016.03.012

Viscoelastic Properties of Human Bladder Tumours

S. C. Barnes[a], B. M. Lawless[a], D. E. T. Shepherd[a,*], D. M. Espino[a], G. R. Bicknell[b], R. T. Bryan[b]

[a]School of Mechanical Engineering, University of Birmingham, B15 2TT

[b]Institute of Cancer & Genomic Sciences, University of Birmingham, B15 2TT

Abstract

The urinary bladder is an organ which facilitates the storage and release of urine. The bladder can develop tumours and bladder cancer is a common malignancy throughout the world. There is a consensus that there are differences in the mechanical properties of normal and malignant tissues. However, the viscoelastic properties of human bladder tumours at the macro scale have not been previously studied. This study investigated the viscoelastic properties of ten bladder tumours, which were tested using dynamic mechanical analysis at frequencies up to 30 Hz. The storage modulus ranged between 0.052 MPa and 0.085 MPa while the loss modulus ranged between 0.019 MPa and 0.043 MPa. Both storage and loss moduli showed frequency dependent behaviour and the storage modulus was higher than the loss modulus for every frequency tested.

Viscoelastic properties may be useful for the development of surgical trainers, surgical devices, computational models and diagnostic equipment.

Keywords

Bladder Cancer; Dynamic Mechanical Analysis; Human; Mechanical Properties; Tumour; Viscoelasticity.

Introduction

The human urinary bladder is a hollow distensible structure located within the pelvis and functioning as the storage organ for urine, thus permitting micturition at socially acceptable times and locations. Urinary bladder cancer is the 4th most common cancer in men and the 13th most common cancer in women in the UK (Cancer Research UK, 2014). Each year 10,200, 123,135 and 72,570 people are diagnosed with bladder cancer in the UK, EU and USA and with mortality of 5,000, 40,252 and 15,210, respectively (Cancer Research UK, 2014; Burger *et al.*, 2013).

In Western populations, over 90% of bladder cancers are transitional cell carcinomas (urothelial carcinomas, urothelial bladder cancer - UBC), and at presentation over 75-85% will be Non-Muscle Invasive Bladder Cancer (NMIBC: stages Ta/T1/Tis), with the remainder being Muscle-Invasive (MIBC: stages T2-4) (Wallace *et al.*, 2002; Lorusso and Silvestris, 2005; van Rhijn *et al.*, 2009; Kaufman *et al.*, 2009). Other types of bladder cancer include squamous cell carcinomas (5%) and adenocarcinomas (>2%) (Kaufman *et al.*, 2009). The cardinal symptom of UBC is painless visible haematuria (presence of blood in the urine), occurring in over 80% of patients at presentation (Wallace *et al.*, 2002; Kaufman *et al.*, 2009) and requiring prompt investigation, most often in a 'haematuria clinic' setting (Lynch *et al.*, 1994). Further investigation of patients suspected of having UBC requires multiple diagnostic procedures, including imaging of the upper urinary tract, urine cytology and cystoscopy (Kaufman *et al.*, 2009; Hollenbeck *et al.*, 2010; Babjuk *et al.*, 2011). In most cases the diagnosis is subsequently confirmed following Transurethral Resection of Bladder Tumour (TURBT) (Kaufman *et al.*, 2009; Babjuk *et al.*, 2011).

Cancers are described by grade and stage. In the UBC setting, grade describes the microscopic appearance of the tumour cells and indicates how biologically aggressive the cells are, with grade 1 (G1) being least aggressive and grade 3 (G3) being most aggressive; alternatively grade can be described as low or high (Mostofi *et al.*, 1973; Epstein *et al.*, 1998; Kaufman *et al.*, 2009). UICC (Union International Contre le Cancer) Tumour Node Metastasis (TNM) staging defines the depth of invasion or other structures that the primary tumour has involved, and also the presence or absence of lymph node and/or distant metastases (Sobin *et al.*, 2009). The architecture of the tumour is classified by its predominant feature; this can be sessile or papillary (Epstein *et al.*, 1998; Remzi *et al.*, 2009). Papillary (pap) describes a tumour with 'finger like' projections (sometimes likened to a sea anemone), as opposed to sessile in which the tumours are solid and flat (Shirai *et al.*, 1989). Tumours can also exhibit both papillary and sessile (mixed) architecture.

NMIBC is typified by a high rate of recurrence (15-61% at one year, depending upon risk category (Sylvester *et al.*, 2006)) and so long-term, even lifelong, surveillance with outpatient flexible cystoscopy is the mainstay of subsequent management (Kaufman *et al.*, 2009; Babjuk *et al.*, 2011). Progression to MIBC (Muscle Invasive Bladder Cancer) is also a concern for high-risk NMIBC patients, occurring in up to 17% of patients at one year (Sylvester *et al.*, 2006). Progression to (or presentation with) muscle-invasive disease (stages T2-4) represents the critical step in the disease course, necessitating more radical therapies and carrying a 5-year survival rate of only 27-50% (Wallace *et al.*, 2002; Advanced Bladder Cancer (ABC) Meta-analysis Collaboration, 2005). For curative intent, patients who present with or progress to MIBC are treated by radiotherapy (Kaufman *et al.*, 2009; Stenzl *et al.*, 2011), chemoradiotherapy (James *et al.*, 2012), radical cystectomy, or neoadjuvant chemotherapy followed by radical cystectomy (Advanced Bladder Cancer (ABC) Meta-analysis

Collaboration, 2005; Kaufman *et al.*, 2009; Stenzl *et al.*, 2011). Consequently, the cumulative cost of treating UBC exceeds all other forms of human cancer. Despite this, there is only modest research funding for UBC compared to other malignancies (Lotan *et al.*, 2009), and as a result there has been a lack of scientific advancement in the field (Lotan *et al.*, 2009; Kaplan *et al.*, 2014).

The mechanical properties of bladder tumours have been rarely studied, despite such data being highly relevant to the development of improved surgical devices, diagnostic tools, computational models and surgical trainers. Previous studies have investigated the Young's modulus (Lekka *et al.*, 1999; Lekka *et al.*, 2001; Lekka *et al.*, 2012) and the shear storage and loss moduli (Abidine *et al.*, 2015) of bladder tumour cells, however these studies only considered the properties at a cellular level but not at the tissue level. Viscoelastic material properties are important as they account for the time dependent nature of a biological tissue's mechanical behaviour. For example the Young's modulus of a tissue will change depending on the loading/strain rate that is applied. The aim of this study was to use Dynamic Mechanical Analysis (DMA) to quantify the frequency-dependent viscoelastic properties of human bladder tumours on the macro scale in terms of storage (*E'*) and loss (*E''*) modulus. Storage modulus characterises the material's ability to elastically store energy whilst the loss modulus characterises the material's ability to dissipate energy (Menard, 2008).

Materials and Methods

Ten human bladder tumour specimens were obtained from 8 patients recruited to the West Midlands (UK) Bladder Cancer Prognosis Programme (BCPP, ethics approval 06/MRE04/65) (Zeegers *et al.*, 2010). All human tissue specimens and data used in this study were collected with informed donor consent in compliance with national and institutional ethical requirements. BCPP methodology and patient characteristics have been described in detail elsewhere (Zeegers *et al.*, 2010; Bryan *et al.*, 2013). Tumour specimens were frozen in liquid nitrogen immediately after removal during TURBT and subsequently stored at -80°C. There is consensus that freezing does not affect the mechanical properties of soft tissues (Chan and Titze, 2003; Szarko *et al.*, 2010; Woo *et al.*, 1986). Before dynamic mechanical testing, the specimens were defrosted in Ringer's solution (Oxoid Ltd, Basingstoke, UK) until thawed. The basic patient and tumour characteristics for each specimen used are provided in table 1, with a representative selection of specimens shown in figure 1.

Each specimen was measured using Vernier callipers (Fisher Scientific, Loughborough, UK) with a precision of 0.1 mm. The specimens were approximated to a cuboid and three measurements for width, depth and height were taken for each specimen. Mean and standard deviation values for these dimensions can be found in table 1.

The specimens were tested using a Bose Electroforce 3200 testing machine, fitted with a 22 N load cell, using WinTest Dynamic Mechanical Analysis (DMA) software (Bose Corporation, Electroforce Systems Group, Minnesota, USA). Other biological and synthetic materials have been tested using Bose testing machines (Fulcher *et al.*, 2009; Gadd and Shepherd, 2011; Millard *et al.*, 2011; Zanetti *et al.*, 2012; Barnes *et al.*, 2015; Patel *et al.*, 2008; Omari *et al.*, 2015). The specimens were compressed using a cylindrical plate with a diameter of 20 mm; the test set-up can be seen in figure 2.

Specimens were tested in a random order chosen using the Excel (2010, Microsoft, Washington, USA) random number function. The specimens were initially given a preload of 0.1 N and were then subjected to a preconditioning cycle of 5 Hz to allow the specimens to stabilise before data

collection (Öhman *et al.*, 2009; Wilcox *et al.*, 2014). After this they were tested from 0.01 to 30 Hz in 14 steps; this was consistent with previous studies on bladder tissue and liver tumours by Barnes *et al*. (2015) and DeWall *et al.* (2012), respectively.

For both the preconditioning cycle and the frequencies 0.01 to 30 Hz the specimens were subjected to a sinusoidally varying displacement (*y*) in the form:

$$y = x + z\sin(2\pi f t) \quad (1)$$

where *x* was the mean displacement (20% of a specimen height; table 1), *z* was the amplitude (0.1*x*), *t* is time (in seconds) and *f* the test frequency. In this instance the amplitude was defined as the peak/trough displacement to the mean displacement.

For example, specimen number 5 had an average height of 3.2 mm which equated to testing parameters of a mean displacement (*x*) of 0.64 mm compression and amplitude (*z*) of 0.064 mm. The values for mean displacement and amplitudes for each specimen can be found in table 2.

Storage (*E'*) and loss (*E''*) moduli were calculated from the displacement sine wave input and load sine wave output using the WinTest DMA software. By using Fourier transforms of the load and displacement data, the software measures the phase angle (δ) between the load and displacement signals and it calculates the dynamic stiffness (*k**) (Barnes *et al.*, 2015). *E'* and *E''* were then calculated from (Fulcher *et al.*, 2009):

$$E' = \frac{k^* cos\delta}{S} \quad (2)$$

$$E'' = \frac{k^* sin\delta}{S} \quad (3)$$

where *S* is the shape factor which was calculated from (Barnes *et al.*, 2015):

$$S = \frac{wd}{h} \quad (4)$$

where *w* is the width, *d* is the depth and *h* is the height of a specimen.

Storage modulus and loss modulus were plotted against frequency and regression analysis was undertaken using Sigma Plot (version 11.0, Systat Software Inc., London, UK). The curve fit relationship was considered significant if $p < 0.05$. The 95% confidence intervals were also generated using Sigma Plot.

Results

Out of the ten specimens studied, the results of three were rejected. Specimen 8 was rejected as the mechanical testing did not induce sufficient load (thus the signal to noise ratio of the measured load was too low for use). The results for specimen 6 were not recorded due to a machine error and for specimen 3 the results were more than 15 standard deviations higher than the mean of the other specimens and it was rejected using Peirce's criterion (Peirce, 1852; Ross, 2003; Patel *et al.*, 2010). For the generation of 95% confidence intervals, the specimen number (n) was taken as 6 because the 7 specimens came from 6 different patients which equated to 6 independent observations (Ranstam, 2012).

The storage modulus was higher than the loss modulus for every frequency of each specimen tested. Storage modulus was found to increase with increasing frequency following a logarithmic trend (figure 4). The trends for the storage modulus (*E'*) against frequency (*f*) were described by the logarithmic curve fit:

$$E' = Aln(f) + B \qquad \text{for } 0.01 \leq f \leq 30 \qquad (5)$$

where *A* and *B* are constants (see table 3 for constants for each specimen). This logarithmic curve fit showed a good correlation to the original data with R^2 values all above 0.7. All relationships were found to be significant ($p < 0.05$).

The mean storage modulus for all specimens against frequency (figure 5) followed the same trend as the individual specimens. The curve fit for the mean storage modulus can be seen in equation 6. From 0.01 Hz to 30 Hz the mean storage modulus increased from 0.05 MPa to 0.085 MPa.

$$E' = 0.0042ln(f) + 0.069 \qquad \text{for } 0.01 \leq f \leq 30 \qquad (6)$$

For individual specimens, the loss modulus was initially at a roughly constant value with increasing frequency until around 1 Hz where the loss modulus started to increase (figure 6). The trends for the loss modulus (*E''*) against frequency (*f*) were described by a second order polynomial curve fit:

$$E'' = C(f^2) + D(f) + E \qquad \text{for } 0.01 \leq f \leq 30 \qquad (7)$$

where *C*, *D* and *E* are constants (see table 3 for constants for each specimen). This polynomial curve fit showed a good correlation with R^2 values all above 0.69. All relationships were found to be significant ($p < 0.05$).

The mean loss modulus for all specimens against frequency (figure 7) followed the same trend as the individual specimens. The curve fit for the mean loss modulus can be seen in equation 8. The mean loss modulus was initially at around 0.02 MPa at frequencies less than or equal to 1 Hz and then increased to 0.043 MPa by 30 Hz.

$$E'' = -0.00003(f^2) + 0.0017(f) + 0.0150 \qquad \text{for } 0.01 \leq f \leq 30 \qquad (8)$$

Discussion

The results of this study show that bladder tumours are viscoelastic throughout the range of frequencies that were tested. Furthermore, the storage modulus was constantly higher than the loss modulus. In comparison to a study by Barnes *et al*. (2015) on the tensile viscoelastic properties of *porcine* bladder where the mean values of storage and loss modulus were 0.36 MPa and 0.05 MPa, respectively, over the same frequency range human bladder tumour had a storage modulus of 0.07 MPa and a loss modulus of 0.02 MPa. In spite of differences in the mammal tested and the type of loading, consistencies in the general trends of the storage and loss modulus were found. At low frequencies (below 1 Hz) the storage modulus of the porcine bladder did show a logarithmic trend similar to the one seen in the results of this study, and the porcine bladder loss modulus showed an increasing trend against frequency (Barnes *et al.*, 2015) which can also be seen in the human bladder tumour results presented here.

DeWall *et al*. (2012) used similar testing equipment and protocols to characterize the viscoelastic properties of normal and tumourous liver tissue. They found that the background (normal) tissue storage modulus was higher than the malignant tissue for each of the frequencies tested. Over a comparable frequency range the storage modulus of the liver tumours (0.01 MPa) was less than the storage modulus found for human bladder tumours in this study (0.08 MPa).

Lekka *et* al. (2012) also found that cancerous cells of a variety of tissue decreased in stiffness in comparison to normal tissue. They reported a value of 0.001 MPa for the Young's modulus of bladder cancer tumours. This study reports a higher value of 0.06 MPa (dynamic modulus) at a comparable loading rate to this study. However, comparison is difficult due to the differences in testing at the cellular and tissue levels and also because dynamic modulus is a viscoelastic property as opposed to Young's modulus which assumes the material to be purely elastic. Dynamic modulus can be calculated from the orthogonal of the storage and loss moduli, $E^* = \sqrt{E'^2 + E''^2}$ (Hukins *et al.*, 1999).

In comparison to a study on the shear dynamic properties of bladder tumour cells by Abidine *et al.* (2015) the axial compressive moduli found in this study were higher at comparable frequencies and both studies presented increasing trends against frequency. This indicates that bladder tumours exhibit higher moduli at the macro scale, however, the studies are difficult to compare due to the differences in testing at the cellular and tissue scales and the differences between shear and compression.

There have also been studies which have looked at tensile testing of *porcine* bladder tissue. Natali *et al.* (2015) investigated the cyclic behaviour of rectangular specimens and found the tissue to exhibit a higher stiffness in the transverse direction. Zanetti *et al.* (2012) also investigated tensile properties and found *porcine* bladder exhibited a secant modulus in the range of 0.1 – 0.45 MPa, at a comparable loading rate this is higher than the dynamic modulus found for human bladder tumour (0.062 MPa). However, comparison between the studies are difficult as: this current study uses human tumours, under compression with dynamic moduli calculated, whereas the studies mentioned above used healthy *porcine* tissue, under tensile testing and calculated a secant modulus.

The translational utility of our findings lie in several areas:

Diagnostic: Ultrasound elastography is effective in the detection of tumours in breast cancer (Gheonea *et al.*, 2011). Elastography makes use of external tissue compression and ultrasound

imaging to map the stiffness of different areas of tissue. The differences in the mechanical properties of normal and tumourous tissue point oncologists to potential regions of malignancy. In breast cancer, malignant tissue is harder and hence stiffer than the surrounding tissue (Itoh *et al.*, 2006). If the moduli for normal and malignant bladder tissue are quantified and significant differences are found, then there is the potential for the application to diagnosis with imaging techniques that use mechanical stimulation; such as ultrasound elastography. Currently such tools are not used in the diagnosis of bladder cancer, but the authors believe that in the future this may become a favourable solution in comparison to cystoscopy, biopsy or cross-sectional imaging.

Surgical training: In applications such as training for surgery, such as TURBT, it may be advantageous for the surgeon to practice or learn to use existing or new (Barnes *et al.*, Submitted) equipment to cut through material with similar viscoelastic properties to tumour tissue. Ahmadzadeh and Hukins (2014) have described a method of manufacturing materials with certain viscoelastic properties that could be used in this instance. The Uro Trainer manufactured by Karl Storz GmbH (Tuttlingen, Germany) is a virtual reality trainer which provides haptic feedback based on the experience of surgeons (Reich *et al.*, 2006). More realistic feedback may be achievable for a range of different tumours with their respective viscoelastic properties.

Instrument design: An indentation system similar to that described by Appleyard *et al* (2001) for cartilage could be manufactured to measure and assess the viscoelastic properties of tumours *in vivo*. The viscoelastic properties of any suspicious bladder tissue or lesions could then be ascertained *in vivo* and these measurements could be used to distinguish between tumorous and healthy tissue; appropriate action could then be taken during the same procedure. This is in contrast to taking a biopsy, waiting for results and then undergoing another procedure.

Computational models: The macro scale values presented in this study would be able to inform better computational models of the bladder. When comparing the behaviour of a healthy bladder to a tumour-containing bladder when subjected to filling, computational methods such as Finite Element Analysis could be used to predict regions with high stress concentrations. Also, Fluid Structure Interaction (FSI) could potentially be used to determine the path of tumour cells during TURBT. Methods for linking fluids and structures have previously been described by Espino *et al.* (2015).

A possible limitation of the current study may be in the shape assumption of a cuboid for the tumour specimens. The majority of the specimens tested had on inspection a rectangular shape, when observing the specimen from above. However, as can be seen in figure 1a and 1b this varied and these specimens were more cylindrical in appearance. The errors in the calculated shape factor are expected to have only a limited effect on the results as the worst case scenario is an overestimation of the shape factor by ~13% when comparing the shape factor of a cuboid to a cylinder. In reality, the shape of the specimens was probably somewhere in between a cuboid and a cylinder so the actual overestimation would have been less. Furthermore, the individual trends for each specimen would not be changed by a difference in shape factor, only offset, as the shape factor was constant for each specimen.

This study made use of unconfined compression; an alternative to this is confined compression. However, its application in relation to human bladder tumours is no more appropriate than unconfined compression; for example, the lateral 'walls' of the tumour are not necessarily confined

by the bladder tissue. Furthermore, during testing there was no evidence of permanent tissue deformation under dynamic loading which can be seen in figure 3 (i.e. a significant volume of fluid is unlikely to have been forced out of the tumour); thus, negating the need for confined compression during testing.

Due to the low sample size, the variables of grade, stage, type, age and gender were not compared. Future studies investigating these variables could be of great value; for example, Swaminathan *et al*. (2011) demonstrated that as ovarian tumour cells become more invasive, their stiffness decreases. Abidine *et al.* (2015) found that the transition frequency of shear storage and loss moduli decreased with increasing invasiveness of bladder cancer cells. It would be of interest to find the transition frequencies at the macro scale, however, there will be difficulties in reaching high enough testing frequencies (some above 200 Hz in the study by Abidine *et al.* (2015)) with uniaxial testing equipment and there may be issues with vibration of soft tissue specimens at these higher frequencies. Furthermore, DeWall *et al*. (2012) have hypothesized that tissue properties may also be useful in diagnosing different tumour types. If there is a relationship between the macro viscoelastic behaviour of bladder tumours and their depth of invasion, grade, stage or type this would be of great value in diagnostic procedures.

Conclusions

It can be concluded that human bladder tumour exhibits frequency dependent viscoelastic properties throughout the range of frequencies tested. The storage modulus exhibited a logarithmically increasing trend against frequency with a mean value of 0.069 MPa and the loss modulus exhibited a quadratic increasing trend against frequency with a mean of 0.027 MPa. Applications of these findings include the diagnosis of bladder cancer, computer simulations of the bladder and the manufacture of more realistic tumour models in surgical trainers.

Acknowledgements

The authors would like to thank Hanna Burton and Hamid Sadeghi for statistical advice and guidance. The authors would also like to thank Carl Hingley, Peter Thornton, Simon Rowan, Jack Garrod and Lee Gauntlet of the School of Mechanical Engineering, University of Birmingham for their technical advice. This study was supported by the Engineering and Physical Sciences Research Council (EP/K502984/1). The equipment used in this study was funded by Arthritis Research UK [Grant number H0671].

We thank all the West Midlands Consultant Urologists and their units involved with BCPP, as well as the BCPP research nurses and Margaret Grant, Deborah Bird, Jennifer Barnwell, Duncan Nekeman and Eline van Roekel.

BCPP is funded by Cancer Research UK, the University of Birmingham and the Birmingham & The Black Country and West Midlands North and South Comprehensive Local Research Networks, and sponsored by the University of Birmingham. The BCPP biospecimen collection is supported by funding from the Birmingham Experimental Cancer Medicine Centre. G Bicknell is funded by a philanthropic donation to the University of Birmingham in support of bladder cancer research.

References

Abidine, Y., Laurent, V.M., Michel, R., Duperray, A., Verdier, C. (2015) Local mechanical properties of bladder cancer cells measured by AFM as a signature of metastatic potential. *European Physical Journal Plus*. **130**(10).

Advanced Bladder Cancer (ABC) Meta-analysis Collaboration (2005) Neoadjuvant chemotherapy in invasive bladder cancer: update of a systematic review and meta-analysis of individual patient data advanced bladder cancer (ABC) meta-analysis collaboration. *European Urology*. **48**, 202–205.

Ahmadzadeh, S.M.H., Hukins, D.W. (2014) Feasibility of using mixtures of silicone elastomers and silicone oils to model the mechanical behaviour of biological tissues. *Proceedings of the Institution of Mechanical Engineers. Part H, Journal of engineering in medicine*. **228**(7), 730–734.

Appleyard, R.C., Swain, M. V, Khanna, S., Murrell, G.A.C. (2001) The accuracy and reliability of a novel handheld dynamic indentation probe for analysing articular cartilage. *Physics in Medicine and Biology*. **46**, 541–550.

Babjuk, M., Oosterlinck, W., Sylvester, R., Kaasinen, E., Böhle, A., Palou-Redorta, J., Rouprêt, M. (2011) EAU guidelines on non-muscle-invasive urothelial carcinoma of the bladder, the 2011 update. *European Urology*. **59**, 997–1008.

Barnes, S.C., Shepherd, D.E.T., Espino, D.M., Bryan, R.T. (2015) Frequency dependent viscoelastic properties of porcine bladder. *Journal of the Mechanical Behavior of Biomedical Materials*. **42**, 168–176.

Barnes, S.C., Shepherd, D.E.T., Espino, D.M., Bryan, R.T., Viney, R., Patel, P. Design of an improved surgical instrument for the removal of bladder tumours. *Submitted to Proceedings of the Institution of Mechanical Engineers, Part H: Journal of Engineering in Medicine*.

Bryan, R.T., Zeegers, M.P., van Roekel, E.H., Bird, D., Grant, M.R., Dunn, J. a, Bathers, S., Iqbal, G., Khan, H.S., Collins, S.I., Howman, A., Deshmukh, N.S., James, N.D., Cheng, K.K., Wallace, D.M.A. (2013) A comparison of patient and tumour characteristics in two UK bladder cancer cohorts separated by 20 years. *BJU International*. **112**(2), 169–75.

Burger, M., Catto, J.W.F., Dalbagni, G., Grossman, H.B., Herr, H., Karakiewicz, P., Kassouf, W., Kiemeney, L. a, La Vecchia, C., Shariat, S., Lotan, Y. (2013) Epidemiology and risk factors of urothelial bladder cancer. *European Urology*. **63**(2), 234–41.

Cancer Research UK (2014) Bladder cancer statistics. [online]. Available from: http://www.cancerresearchuk.org/cancer-info/cancerstats/keyfacts/bladder-cancer/uk-bladder-cancer-statistics [Accessed December 16, 2014].

Chan, R.W., Titze, I.R. (2003) Effect of postmortem changes and freezing on the viscoelastic properties of vocal fold tissues. *Annals of Biomedical Engineering*. **31**(4), 482–491.

DeWall, R.J., Bharat, S., Varghese, T., Hanson, M.E., Agni, R.M., Kliewer, M.A. (2012) Characterizing the compression-dependent viscoelastic properties of human hepatic pathologies using dynamic compression testing. *Physics in Medicine and Biology*. **57**, 2273–2286.

Epstein, J., Amin, M., Reuter, V., Mosotofi, F. (1998) The World Health Organization/International Society of Urological Pathology consensus on classification of urothelial (transitional cell) neoplasms of the urinary bladder. *The American Journal of Surgical Pathology*. **22**(12), 1435–1448.

Espino, D.M., Shepherd, D.E.T., Hukins, D.W.L. (2015) Transient large strain contact modelling: A comparison of contact techniques for simultaneous fluid–structure interaction. *European Journal of Mechanics - B/Fluids*. **51**, 54–60.

Fulcher, G.R., Hukins, D.W.L., Shepherd, D.E.T. (2009) Viscoelastic properties of bovine articular cartilage attached to subchondral bone at high frequencies. *BMC Musculoskeletal Disorders*. **10**, 61.

Gadd, M.J., Shepherd, D.E.T. (2011) Viscoelastic properties of the intervertebral disc and the effect of nucleus pulposus removal. *Proceedings of the Institution of Mechanical Engineers, Part H: Journal of Engineering in Medicine*. **225**(4), 335–341.

Gheonea, I.A., Stoica, Z., Bondari, S. (2011) Differential diagnosis of breast lesions using ultrasound elastography. *The Indian Journal of Radiology & Imaging*. **21**(4), 301–5.

Hollenbeck, B.K., Dunn, R.L., Ye, Z., Hollingsworth, J.M., Skolarus, T.A., Kim, S.P., Montie, J.E., Lee, C.T., Wood, D.P., Miller, D.C. (2010) Delays in diagnosis and bladder cancer mortality. *Cancer*. **116**(22), 5235–5242.

Hukins, D.W.L., Leahy, J.C., Mathias, K.J. (1999) Biomaterials: defining the mechanical properties of natural tissues and selection of replacement materials. *Journal of Materials Chemistry*. **9**(3), 629–636.

Itoh, A., Ueno, E., Tohno, E., Kamma, H., Takahashi, H., Shiina, T., Yamakawa, M., Matsumura, T. (2006) Breast disease: clinical application of US elastography for diagnosis. *Radiology*. **239**(2), 341–350.

James, N., Hussain, S., Hall, E., Tremlett, J., Rawlings, C., Crundwell, M., Sizer, B., Screenivasan, T., Hendron, C., Lewis, R., Waters, R., Huddart, R. (2012) Radiotherapy with or without chemotherapy in muscle-invasive bladder cancer. *The New England Journal of Medicine*. **366**(16), 1477–1488.

Kaplan, A., Litwin, M., Chamie, K. (2014) The future of bladder cancer care in the USA. *Nature Reviews Urology*. **11**, 59–62.

Kaufman, D.S., Shipley, W.U., Feldman, A.S. (2009) Bladder cancer. *Lancet*. **374**(9685), 239–49.

Lekka, M., Laidler, P., Gil, D., Lekki, J., Stachura, Z., Hrynkiewicz, A.Z. (1999) Elasticity of normal and cancerous human bladder cells studied by scanning force microscopy. *European Biophysics Journal*. **28**(4), 312–316.

Lekka, M., Laidler, P., Ignacak, J.J., Labd, M., Lekki, J., Struszczyk, H., Stachura, Z., Hrynkiewicz, A.Z. (2001) The effect of chitosan on stiffness and glycolytic activity of human bladder cells. *Biochimica et Biophysica Acta - Molecular Cell Research*. **1540**(2), 127 – 136.

Lekka, M., Pogoda, K., Gostek, J., Klymenko, O., Prauzner-Bechcicki, S., Wiltowska-Zuber, J., Jaczewska, J., Lekki, J., Stachura, Z. (2012) Cancer cell recognition - Mechanical phenotype. *Micron*. **43**(12), 1259–1266.

Lorusso, V., Silvestris, N. (2005) Systemic chemotherapy for patients with advanced and metastatic bladder cancer: current status and future directions. *Annals of Oncology - English Edition*. **16**(4), 85–89.

Lotan, Y., Kamat, A.M., Porter, M.P., Robinson, V.L., Shore, N., Jewett, M., Schelhammer, P.F., White, R.D., Quale, D., Lee, C.T. (2009) Key concerns about the current state of bladder cancer: a position paper from the bladder cancer think tank, the bladder cancer advocacy network, and the society of urologic oncology. *Cancer*. **115**(18), 4096–4103.

Lynch, T., Waymont, B., Dunn, J., Begum, G., Bathers, S. (1994) Rapid diagnostic service for patients with haematuria. *British Journal of Urology*. **73**(2), 147–151.

Menard, K. (2008) *Dynamic mechanical analysis*. Boca Raton: CRC Press Taylor & Francis Group.

Millard, L., Espino, D.M., Shepherd, D.E.T., Hukins, D.W.L., Buchan, K.G. (2011) Mechanical properties of chordae tendineae of the mitral heart valve: young's modulus, structural stiffness, and effects of aging. *Journal of Mechanics in Medicine and Biology*. **11**(1), 221–230.

Mostofi, F., Sobin, L., Torloni, H. (1973) Histological typing of urinary bladder tumours. *International Histological Classification of Tumors; No. 10. Geneva, Switzerland: World Health Organization*, 15–17.

Natali, A.N., Audenino, A.L., Artibani, W., Fontanella, C.G., Carniel, E.L., Zanetti, E.M. (2015) Bladder tissue biomechanical behavior: experimental tests and constitutive formulation. *Journal of Biomechanics*. **48**(12), 3088–3096.

Öhman, C., Baleani, M., Viceconti, M. (2009) Repeatability of experimental procedures to determine mechanical behaviour of ligaments. *Acta of Bioengineering and Biomechanics*. **11**(1), 19–23.

Omari, E.A., Varghese, T., Kliewer, M.A., Harter, J., Hartenbach, E.M. (2015) Dynamic and quasi-static mechanical testing for characterization of the viscoelastic properties of human uterine tissue. *Journal of Biomechanics*. **48**(10), 1–7.

Patel, P.S.D., Shepherd, D.E.T., Hukins, D.W.L. (2008) Compressive properties of commercially available polyurethane foams as mechanical models for osteoporotic human cancellous bone. *BMC Musculoskeletal Disorders*. **9**, 137.

Patel, P.S.D., Shepherd, D.E.T., Hukins, D.W.L. (2010) The effect of screw insertion angle and thread type on the pullout strength of bone screws in normal and osteoporotic cancellous bone models. *Medical Engineering and Physics*. **32**(8), 822–828.

Peirce, B. (1852) Criterion for the rejection of doubtful observations. *The Astronomical Journal*. **2**, 161 – 163.

Ranstam, J. (2012) Repeated measurements, bilateral observations and pseudoreplicates, why does it matter? *Osteoarthritis and Cartilage*. **20**(6), 473–475.

Reich, O., Noll, M., Gratzke, C., Bachmann, A., Waidelich, R., Seitz, M., Schlenker, B., Baumgartner, R., Hofstetter, A., Stief, C.G. (2006) High-level virtual reality simulator for endourologic procedures of lower urinary tract. *Urology*. **67**(6), 1144–1148.

Remzi, M., Haitel, A., Margulis, V., Karakiewizc, P., Montorsi, F., Kikuchi, E., Zigeuner, R., Weizer, A., Bolenz, C., Bensalah, K., Suardi, N., Raman, J.D., Lotan, Y., Waldert, M., Ng, C.K., Fernández, M., Koppie, T.M., Ströbel, P., Kabbani, W., Murai, M., Langner, C., Roscigno, M., Wheat, J., Guo, C.C., Wood, C.G., Shariat, S.F. (2009) Tumour architecture is an independent predictor of outcomes after nephroureterectomy: A multi-institutional analysis of 1363 patients. *BJU International*. **103**(3), 307–311.

van Rhijn, B.W.G., Burger, M., Lotan, Y., Solsona, E., Stief, C.G., Sylvester, R.J., Witjes, J.A., Zlotta, A.R. (2009) Recurrence and progression of disease in non-muscle-invasive bladder cancer: from epidemiology to treatment strategy. *European Urology*. **56**(3), 430–42.

Ross, S.M. (2003) Peirce's criterion for the elimination of suspect experimental data. *Journal of Engineering Technology*. **20**(2), 38–41.

Shirai, T., Fukushima, S., Tagawa, Y., Sturai, T., Okumura, M., Ito, N. (1989) Cell proliferation induced by uracil-calculi and subsequent development of reversible papillomatosis in the rat urinary bladder. *Cancer Research*. **49**(2), 378–383.

Sobin, L.H., Gospodarowicz, M.K., Wittekind, C. (2009) *TNM classification of malignant tumours*. 7th ed. Oxford: Wiley-Blackwell.

Stenzl, A., Cowan, N.C., De Santis, M., Kuczyk, M. a., Merseburger, A.S., Ribal, M.J., Sherif, A., Witjes, J.A. (2011) Treatment of muscle-invasive and metastatic bladder cancer: update of the EAU guidelines. *European Urology*. **59**(6), 1009–1018.

Swaminathan, V., Mythreye, K., Tim O'Brien, E., Berchuck, A., Blobe, G.C., Superfine, R. (2011) Mechanical Stiffness grades metastatic potential in patient tumor cells and in cancer cell lines. *Cancer Research*. **71**(15), 5075–5080.

Sylvester, R.J., van der Meijden, A.P.M., Oosterlinck, W., Witjes, J.A., Bouffioux, C., Denis, L., Newling, D.W.W., Kurth, K. (2006) Predicting recurrence and progression in individual patients with stage Ta T1 bladder cancer using EORTC risk tables: a combined analysis of 2596 patients from seven EORTC trials. *European Urology*. **49**(3), 466–477.

Szarko, M., Muldrew, K., Bertram, J.E. (2010) Freeze-thaw treatment effects on the dynamic mechanical properties of articular cartilage. *BMC Musculoskeletal Disorders*. **11**, 231.

Wallace, D., Bryan, R., Dunn, J., Begum, G., Bathers, S. (2002) Delay and survival in bladder cancer. *BJU International*. **89**(9), 868–878.

Wilcox, A.G., Buchan, K.G., Espino, D.M. (2014) Frequency and diameter dependent viscoelastic properties of mitral valve chordae tendineae. *Journal of the Mechanical Behavior of Biomedical Materials*. **30**, 186–95.

Woo, S.L., Orlando, C.A., Camp, J.F., Akeson, W.H. (1986) Effects of postmortem storage by freezing on ligament tensile behavior. *Journal of Biomechanics*. **19**(5), 399–404.

Zanetti, E.M., Perrini, M., Bignardi, C., Audenino, A.L. (2012) Bladder tissue passive response to monotonic and cyclic loading. *Biorheology*. **49**(1), 49–63.

Zeegers, M.P., Bryan, R.T., Langford, C., Billingham, L., Murray, P., Deshmukh, N.S., Hussain, S., James, N., Wallace, D.M.A., Cheng, K.K. (2010) The West Midlands bladder cancer prognosis programme: rationale and design. *BJU International*. **105**(6), 784–788.

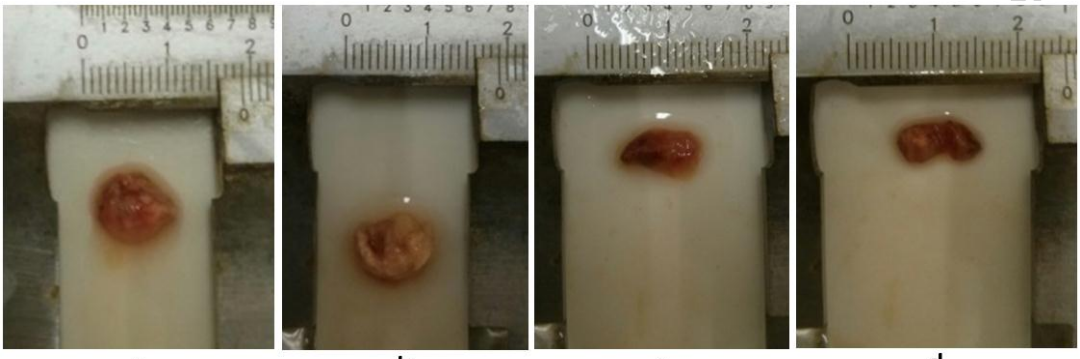

Figure 1 – Human bladder tumour specimens: (a) specimen 2; (b) specimen 3; (c) specimen 6; (d) specimen 7.

Figure 2 – Compressive DMA set-up for human bladder tumours.

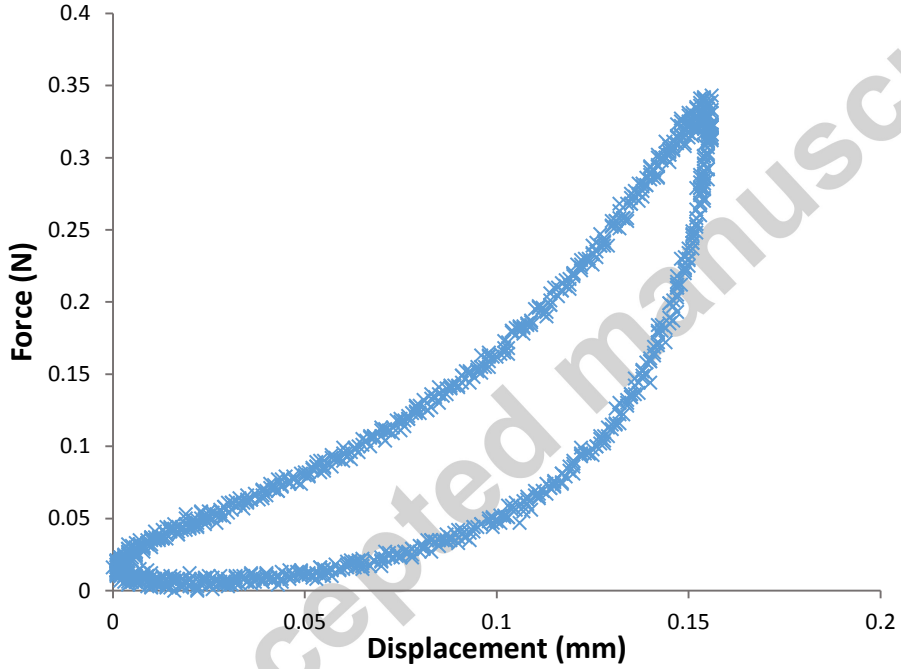

Figure 3 – Load displacement data for specimen 9 at 2 Hz.

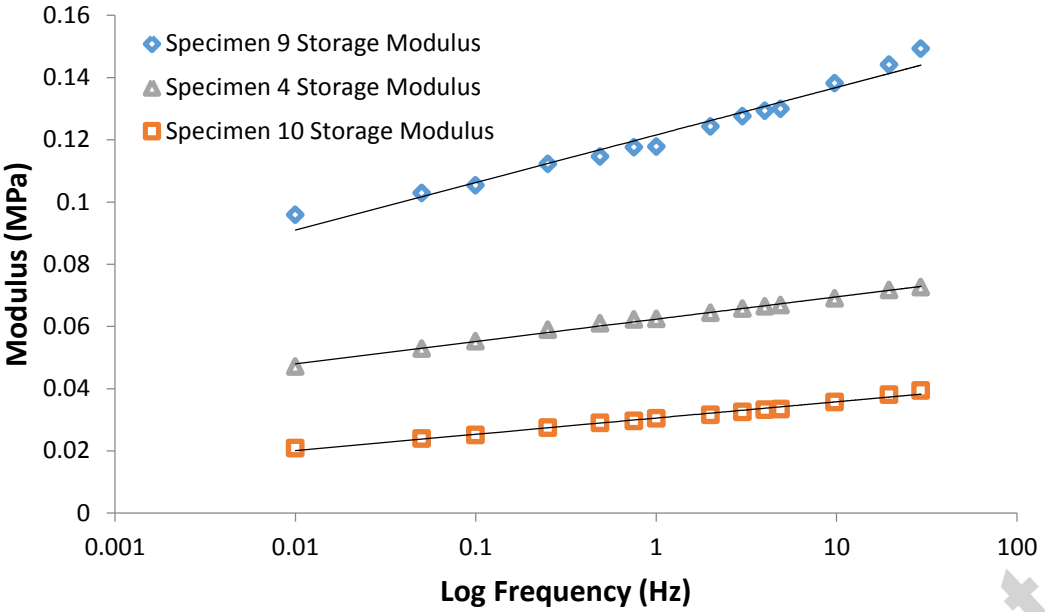

Figure 4 – Storage modulus (*E'*) against log frequency (*f*) for three individual tumour specimens. The curve fit is given by equation 5.

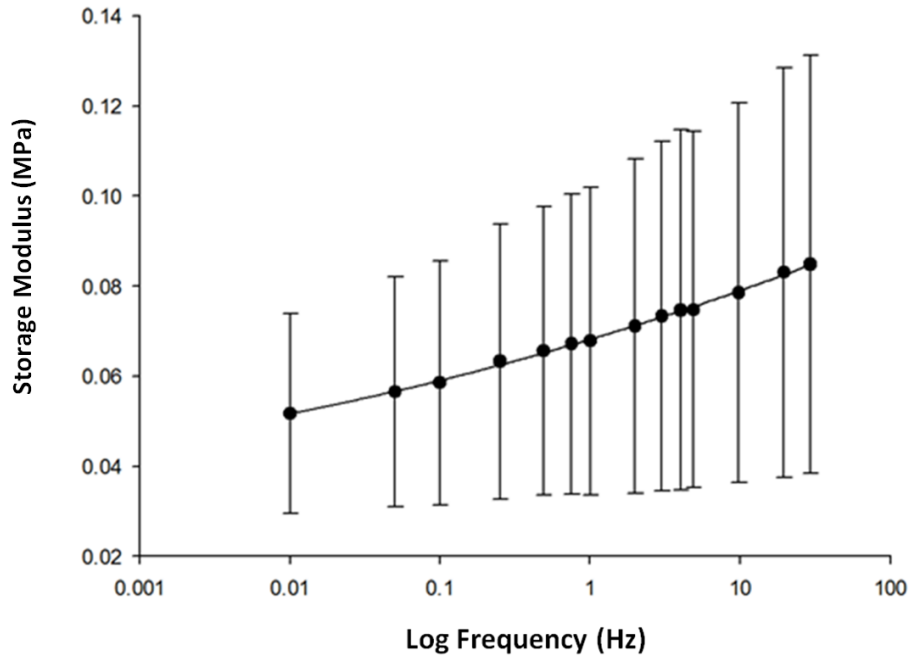

Figure 5 – Mean storage modulus (*E'*) against log frequency (*f*). Error bars represent the 95% confidence intervals for the sample. The mean curve fit for the storage modulus against log frequency is stated in equation 6. Mean storage modulus across all frequencies tested was 0.069 MPa.

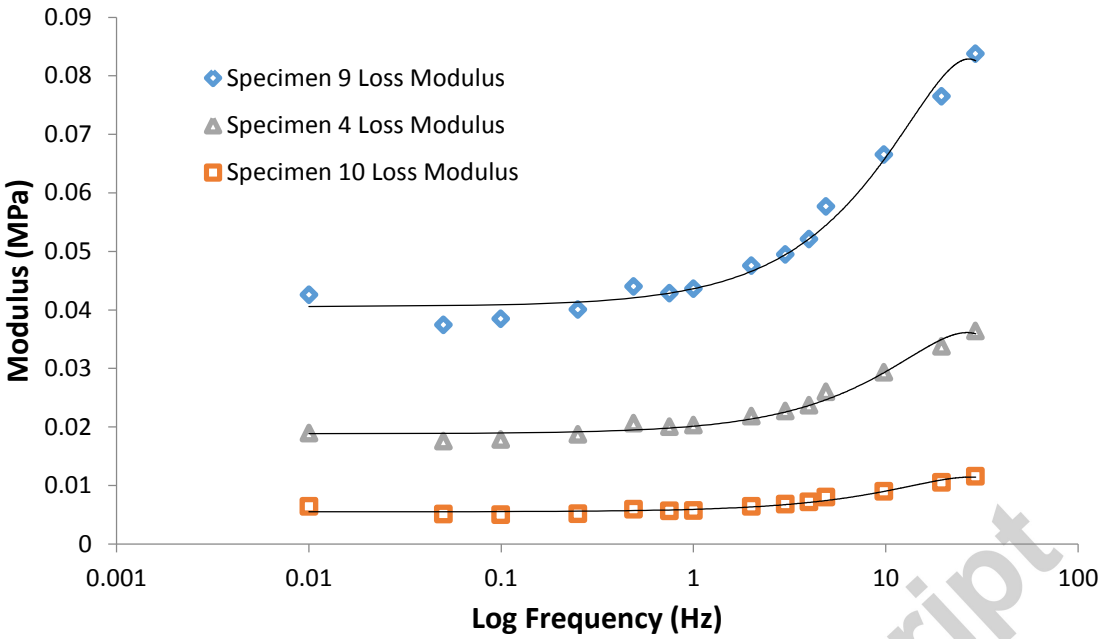

Figure 6 – Loss modulus (*E''*) against log frequency (*f*) for three individual tumour specimens. The curve fit is given by equation 8.

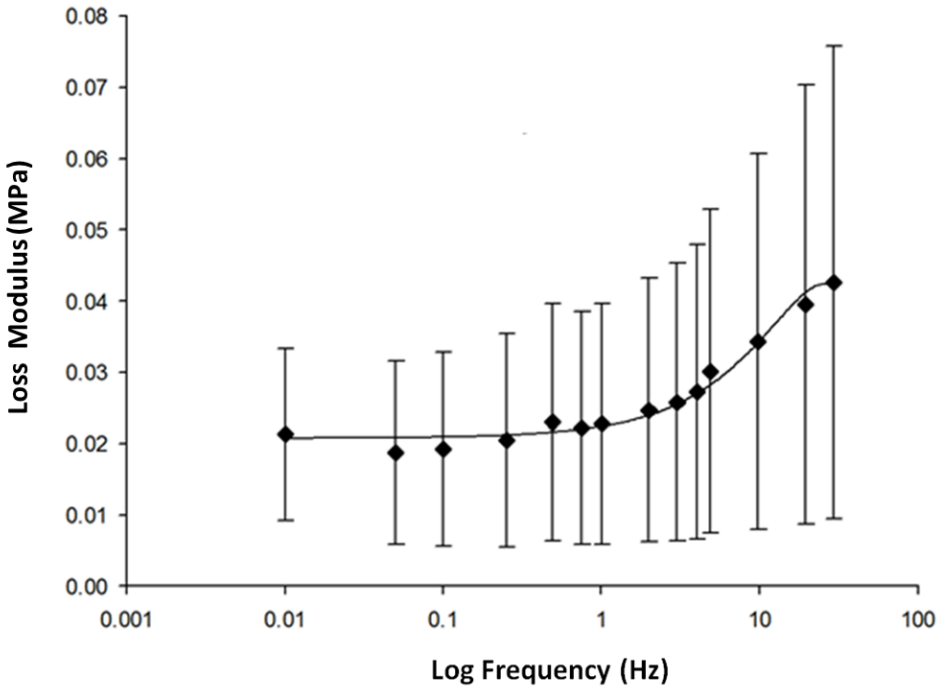

Figure 7 – Mean loss modulus (*E''*) against log frequency (*f*). Error bars represent 95% confidence intervals for the sample. The mean curve fit for the storage modulus against log frequency is stated in equation 8. Mean loss modulus across all frequencies tested was 0.027 MPa.

Table 1 - Individual information for the 10 bladder tumour specimens. Three of the specimens used (2, 6 & 7) were from the same individual. SD refers to standard deviation.

Specimen Number	Grade/ Stage	Architecture	Age at collection	Gender	Mean Dimensions (SD)		
					Width (mm)	Depth (mm)	Height (mm)
1	Non-UBC	pap	83	Male	5.4 (0.2)	5.5 (0.5)	3.1 (0.2)
2	G3pT2+	pap	72	Male	8.1 (1.5)	7.5 (0.7)	5.0 (0.2)
3	G1pTa	pap	62	Male	3.8 (0.2)	4.9 (0.5)	3.0 (0.5)
4	G3pT2+	mixed	90	Female	12.5 (2.6)	8.1 (1.1)	5.2 (0.4)
5	Non-UBC	mixed	73	Female	4.4 (1.3)	7.6 (0.6)	3.2 (0.2)
6	G3pT2+	pap	72	Male	3.9 (0.4)	6.8 (1.4)	3.0 (0.2)
7	G3pT2+	pap	72	Male	6.2 (0.3)	18.3 (0.2)	4.8 (0.4)
8	G2pT1	pap	73	Male	3.2 (0.1)	6.6 (0.3)	1.0 (0.2)
9	G3pT2+	mixed	68	Female	5.3 (1.0)	10.5 (1.8)	3.9 (0.4)
10	G3pT2+	pap	83	Male	4.7 (1.0)	9.8 (0.9)	2.8 (1.5)

Table 2 – Human bladder tumour testing parameters.

Specimen Number	Testing Parameters	
	Mean Displacement (mm)	Amplitude (mm)
1	0.613	0.061
2	1.007	0.101
3	0.600	0.060

4	1.033	0.103
5	0.640	0.064
6	0.593	0.059
7	0.953	0.095
8	0.207	0.021
9	0.780	0.078
10	0.567	0.057

Table 3 – Curve fit results for storage and loss modulus. All coefficients were found to be statistically significant (p<0.05)

Specimen Number	Storage Modulus Curve Fit (E'=A*ln(f)+B)			Loss Modulus Curve Fit (E''=Cf^2+Df+E)			
	A	B	R^2	C (x10^{-3})	D	E	R^2
1	0.0132	0.1200	0.997	-0.107	0.0050	0.0045	0.953
2	0.0017	0.0365	0.865	-0.016	0.0008	0.0098	0.939
3	0.0031	0.0624	0.995	-0.025	0.0013	0.0188	0.981
4	0.0012	0.0641	0.848	-0.016	0.0008	0.0167	0.904
5	0.0013	0.0481	0.705	-0.007	0.0004	0.0093	0.691
6	0.0066	0.1216	0.966	-0.058	0.0031	0.0406	0.982
7	0.0023	0.0306	0.989	-0.008	0.0004	0.0055	0.960
Mean	0.0042	0.0690	0.909	-0.03	0.0017	0.0150	0.916